

One-Dimensional Polymers Based on $[\{\text{CpMo}(\text{CO})_2\}_2(\mu, \eta^2\text{-P}_2)]$: Solid-State Conformation Analysis by NMR Spectroscopy and DFT Calculations

Manfred Scheer,^{*[a]} Laurence Gregoriades,^[a] Junfeng Bai,^[a, b] Marek Sierka,^[c] Gunther Brunklaus,^[d] and Hellmut Eckert^{*[d]}

Dedicated to Prof. M. Jansen on the occasion of his 60th birthday

Abstract: Reaction of the complex $[\{\text{CpMo}(\text{CO})_2\}_2(\mu, \eta^2\text{-P}_2)]$ (**1**) with Cu^I halides leads to the quantitative formation of the novel one-dimensional linear polymers $[\text{CuX}\{\text{Cp}_2\text{Mo}_2(\text{CO})_4(\mu, \eta^2:\eta^1:\eta^1\text{-P}_2)\}]_\infty$ (X = Cl (**4**), Br (**5**), I (**6**)). The same products **4** and **5** were obtained when **1** was treated with CuCl₂ and CuBr₂, respectively. The

solid-state structures are compared and their remarkable influence on the respective ³¹P magic angle spinning

Keywords: density functional calculations • molybdenum • NMR spectroscopy • phosphorus • polymers • solid-state structures

(MAS) NMR spectra is interpreted with the help of density functional theory (DFT) calculations on the model compounds $[\{(\text{CuX})_2\{\text{Cp}_2\text{Cr}_2(\text{CO})_4(\mu, \eta^2:\eta^1:\eta^1\text{-P}_2)\}_2\}]_3$ (X = Cl (**4a**), Br (**5a**)) in which the molybdenum atoms are replaced by their lighter homologue chromium.

Introduction

Self-organisation of discrete units to form supramolecular aggregates and networks is a prominent field in contemporary chemistry.^[1] In contrast to common methodologies in this field which use N- and O-donor-containing ligands, respectively, to connect different metal centres, our goal is to employ P_n-ligand complexes as connecting moieties for the

formation of discrete oligomeric assemblies as well as one-dimensional (1D) and two-dimensional (2D) polymers.

One of our approaches in this field makes use of the complex $[\{\text{CpMo}(\text{CO})_2\}_2(\mu, \eta^2\text{-P}_2)]$ (**1**) as a linking unit between Cu^I and Ag^I centres.^[2] For example, the reaction of **1** with Ag(CF₃SO₃) yields the soluble oligomeric dicationic species $[\text{Ag}_2\{\{\text{Cp}_2\text{Mo}_2(\text{CO})_4(\mu, \eta^2:\eta^1:\eta^1\text{-P}_2)\}_2\}\{\text{Cp}_2\text{Mo}_2(\text{CO})_4(\mu, \eta^2:\eta^1:\eta^1\text{-P}_2)\}_2][\text{CF}_3\text{SO}_3]_2$ (**2**), whereas the reaction with AgNO₃ leads to the formation of the undulated 1D polymer $[\text{Ag}_2\{\text{Cp}_2\text{Mo}_2(\text{CO})_4(\mu, \eta^2:\eta^1:\eta^1\text{-P}_2)\}_3(\mu, \eta^1:\eta^1\text{-NO}_3)]_\infty[\text{NO}_3]_\infty$ (**3**).

The reaction of **1** with CuBr gives a novel linear 1D-polymer,^[2] a synthetic concept which has been now extended to the complete series of Cu^I as well as Cu^{II} halides (excluding CuF₂). The synthesis, solid-state structures and the surprising ³¹P MAS-NMR features of the compounds $[\text{Cu}(\mu\text{-X})\{\text{Cp}_2\text{Mo}_2(\text{CO})_4(\mu, \eta^2:\eta^1:\eta^1\text{-P}_2)\}]_\infty$ (X = Cl (**4**), Br (**5**), I (**6**)) resulting from apparently small differences in the orientations of the ligands within the infinite structures of the compounds, are reported herein.

Results and Discussion

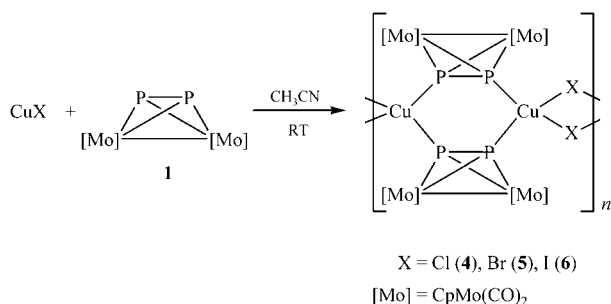
The reaction of **1** with the appropriate Cu^I halide in CH₃CN (Scheme 1) results in the immediate formation of the corresponding 1D polymers **4–6** in high yields. Complexes **4–6** are red crystalline solids that are air- and light-sensitive and

[a] Prof. Dr. M. Scheer, MChem. L. Gregoriades, Dr. J. Bai
Institut für Anorganische Chemie der Universität Regensburg
93040 Regensburg (Germany)
Fax: (+49)941-943-4441
E-mail: mascheer@chemie.uni-regensburg.de

[b] Dr. J. Bai
Present address: Coordination Chemistry Institute &
The State Key Laboratory of Coordination Chemistry
Nanjing University, 210093 Nanjing (P. R. China)

[c] Dr. M. Sierka
Institut für Physikalische Chemie
der Humboldt-Universität zu Berlin
Brook-Taylor-Str. 2, 12489 Berlin (Germany)

[d] Dr. G. Brunklaus, Prof. Dr. H. Eckert
Institut für Physikalische Chemie der Universität Münster
Corrensstr. 30, 48149 Münster (Germany)
Fax: (+49)253-83-29159
E-mail: eckerth@uni-muenster.de



Scheme 1. Preparation of the polymers **4–6**.

insoluble in common solvents. In the IR spectra of all the compounds, CO stretching frequencies attributable to terminal CO ligands are observed.

In an effort to synthesise supramolecular species with novel structural motifs, compound **1** was also treated with CuCl₂ and CuBr₂. A solution of the appropriate Cu^{II} halide in CH₃CN was mixed slowly with a solution of **1** in toluene, yielding dark red needle-shaped crystals within a week. X-ray crystallographic analysis revealed that the products are identical to those resulting from the reaction of the appropriate Cu^I halide with **1**, thus indicating reduction of the Cu^{II} complexes. The yields, which approach 50%, suggest that this reduction is essentially quantitative. Attempts to establish the nature and identity of the oxidation products were inconclusive.

Single crystals of the products **4–6**, grown by layering a solution of the appropriate Cu^I halide in CH₃CN over a solution of **1** in CH₃CN, were examined by X-ray crystallography; details of the measurements are summarised in Table 1.

Table 1. Crystallographic data for compounds **4** and **6**.

	4	6 (CH ₃ CN) _∞
formula	C ₁₄ H ₁₀ ClCuMo ₂ O ₄ P ₂	C ₁₆ H ₁₃ CuIMo ₂ NO ₄ P ₂
<i>M_r</i>	595.03	727.53
crystal size [mm]	0.25 × 0.12 × 0.03	0.20 × 0.10 × 0.01
<i>T</i> [K]	203(2)	210(2)
crystal system	monoclinic	triclinic
space group	<i>C2/c</i>	<i>P</i> $\bar{1}$
<i>a</i> [Å]	25.751(5)	8.0530(16)
<i>b</i> [Å]	8.032(2)	11.498(2)
<i>c</i> [Å]	17.329(4)	11.647(2)
α [°]	90	83.22(3)
β [°]	93.32(3)	82.34(3)
γ [°]	90	77.81(3)
<i>V</i> [Å ³]	3578.2(1)	1040.2(4)
<i>Z</i>	8	2
ρ_{calcd} [g cm ⁻³]	2.209	2.323
μ (AgK α) [mm ⁻¹]	5.958	5.849
θ range [°]	2.10–20.00	2.10–24.06
reflns collected/unique	7440/2753	13222/6230
obsvd reflns with $[I > 2\sigma(I)]$	2753	5135
<i>R</i> _{int}	0.0691	0.0442
GOF on <i>F</i> ²	1.006	1.034
final <i>R</i> indices [$I > 2\sigma(I)$]	<i>R</i> ₁ = 0.0449 <i>wR</i> ₂ = 0.1068	<i>R</i> ₁ = 0.0381 <i>wR</i> ₂ = 0.0951
<i>R</i> indices (all data)	<i>R</i> ₁ = 0.0657 <i>wR</i> ₂ = 0.1188	<i>R</i> ₁ = 0.0496 <i>wR</i> ₂ = 0.1019
max/min $\Delta\rho$ [e Å ⁻³]	1.321/–1.044	0.932/–1.373

Selected bond lengths and angles for **4**, **5**, and **6** are given in Table 2. Compounds **4** (Figure 1) and **5** (Figure 2) crystallise in the monoclinic space groups *C2/c* and *P2₁/n*, respectively.^[3] The iodide derivative **6** (Figure 3) crystallises in the triclinic space group *P* $\bar{1}$ and contains one molecule of CH₃CN per formula unit in the crystal lattice. In all the compounds,

Table 2. Comparison of selected bond lengths [Å] and angles [°] for **4**, **5** and **6**.

	4	5	6
P–P	2.075(2)	2.079(2)	2.080(2)
Cu–P	2.282(2), 2.304(2)	2.294(2), 2.300(2)	2.312(1)
Cu–X	2.348(2), 2.360(2)	2.472(1), 2.481(1)	2.606(1), 2.668(1)
P–Cu–P	99.69(9), 103.81(9)	102.28(6)	105.09(5)
P–P–Cu	126.04(8), 131.89(9)	125.79(8), 131.71(8)	121.13(6), 133.62(6)
Cu–X–Cu	81.33(7)	77.80(4)	74.83(3)
X–Cu–X	98.31(9), 99.03(1)	102.20(4)	105.17(3)

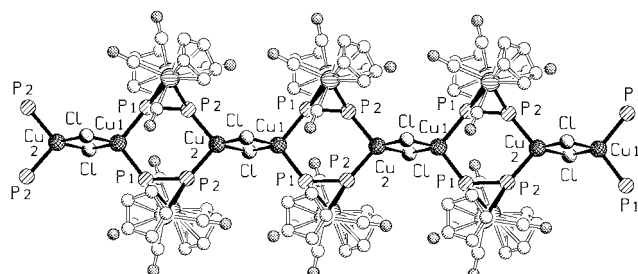


Figure 1. View of the 1D linear chain of **4** (hydrogen atoms are omitted for clarity).

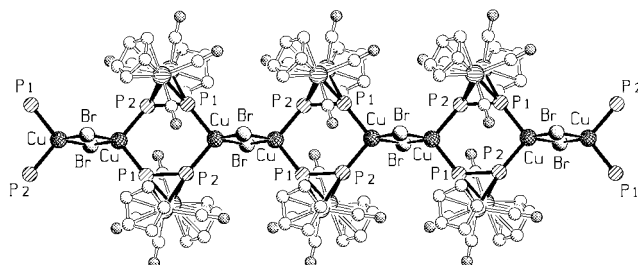


Figure 2. View of the 1D linear chain of **5** (hydrogen atoms are omitted for clarity).

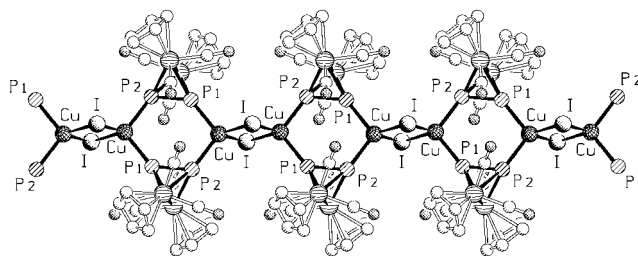


Figure 3. View of the 1D linear chain of **6** (hydrogen atoms are omitted for clarity).

the coordination geometry around the Cu atoms is a distorted tetrahedron and the Mo_2P_2 moieties remain essentially unchanged compared with the Mo_2P_2 core in **1**.^[4] In **4–6** the phosphorus atoms of **1** bridge the Cu^{I} atoms to form a structure consisting of an alternating arrangement of six-membered Cu_2P_4 and nearly orthogonally oriented four-membered Cu_2X_2 rings.

The P–P bond lengths of the P_2 units in **4–6** are 2.075(2), 2.079(2) and 2.080(2) Å, respectively, which are similar to those in the uncoordinated complex **1** (2.079(2) Å)^[4] and the compound $[\{\text{Re}(\text{CO})_3\text{Br}\}_2\{\{\text{Cp}_2\text{Mo}_2(\text{CO})_4(\mu,\eta^2-\eta^1-\eta^1-\text{P}_2)\}_2\}]$ (2.071(9) Å),^[5] but marginally shorter than those in the complexes **2** (2.098(2) and 2.137(2) Å) and **3** (2.097(2) and 2.099(2) Å).^[2] The lengths of the Cu–P bonds in **4** (2.282(2) and 2.304(2) Å) and **5** (2.294(2) and 2.300(2) Å) are slightly shorter than those in $[\{(\text{triphos})\text{CoP}_3\}_2\text{Cu}]\text{PF}_6$ (triphos = 1,1,1-tris(diphenylphosphanylmethyl)ethane; 2.303(2)–2.360(2) Å),^[6] whereas those of **6** (2.312(1) Å) lie within this range. The Cu–X bond lengths (2.348(2) and 2.360(2) Å (**4**); 2.472(1) and 2.481(1) Å (**5**); 2.606(1) and 2.668(1) Å (**6**)) are within the range of those reported for the compounds $[\text{Cu}_2(\text{PPh}_3)_3\text{X}_2]$ (X = Cl^[7] 2.247(4)–2.454(4) Å, Br^[8] 2.370(2)–2.610(2) Å, I^[9] 2.500(2)–2.819(1) Å).

The structures of the polymer cores are compared in Figure 4. By viewing the polymers perpendicular to the faces of their planar Cu_2X_2 rings it can be seen that in **4** the Cu atoms form a linear arrangement ($\text{Cu}\cdots\text{Cu}\cdots\text{Cu}$ 180.00(1)°) whereas in **5** and **6** the Cu atoms are alternately distributed along two parallel lines ($\text{Cu}\cdots\text{Cu}\cdots\text{Cu}$ 177.33(1)° (**5**), 169.24(1)° (**6**)). The Cu_2P_4 rings in **4** are twisted along the $\text{Cu}\cdots\text{Cu}$ axis and as a result the P1 and P2 atoms are ar-

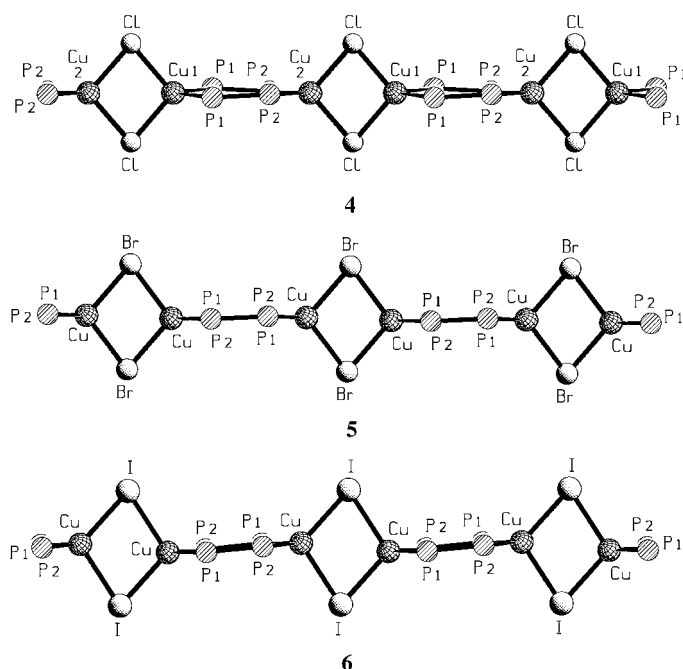


Figure 4. View of polymers **4**, **5** and **6** perpendicular to the faces of the Cu_2X_2 rings (Mo atoms and their supporting ligands are omitted for clarity).

ranged in an alternating fashion above and below the plane that contains the Cu atoms, which in turn is perpendicular to that defined by the Cu_2X_2 rings (P1 ± 0.054 Å, P2 ± 0.056 Å, mean deviation from plane 0.037 Å). Opposite angles within these rings are not equal (P1–P2–Cu2 131.89(9)°; P2–P1–Cu1 126.04(8)°; P1–Cu1–P1 103.81(9)°; P2–Cu2–P2 99.69(9)°). In polymers **5** and **6**, the Cu_2P_4 rings adopt a chairlike conformation (angle between Cu–P1–P2 and P1–P2–P1–P2 planes: 176.1° (**5**), 176.6° (**6**)) and opposite angles within these rings are equal (P1–P2–Cu 131.71(8)° (**5**), 121.13(6)° (**6**); P2–P1–Cu 125.79(8)° (**5**), 133.62(6)° (**6**); P1–Cu–P2 102.28(6)° (**5**), 105.09(5)° (**6**)).

As the size of the halogen atom increases, the angles P–Cu–P and X–Cu–X (X = Cl 98.31(9) and 99.03(1)°, Br 102.20(4)°, I 105.17(3)°) increase, while there is a successive decrease in the angles Cu–X–Cu (X = Cl 81.33(7)°, Br 77.80(4)°, I 74.83(3)°). It is also interesting to note the change in the Cu \cdots Cu interatomic distances in the Cu_2X_2 rings (X = Cl 3.068(1) Å, Br 3.095(1) Å, I 3.205(1) Å) and in the Cu_2P_4 units (X = Cl 4.964(1) Å, Br 4.955(1) Å, I 4.882(1) Å).

The experimental and fitted ^{31}P MAS-NMR spectra of the compounds **4–6** are illustrated in Figures 5–7. While the spectrum of the CuI polymer **6** displays a broad signal centred at about –87 ppm, each of the spectra of **4** and **5** display two distinct multiplets about 150 ppm apart. The multiplets arise from the combined effect of homonuclear 1J (^{31}P , ^{31}P) and heteronuclear 1J ($^{63/65}\text{Cu}$, ^{31}P) indirect spin–spin interactions. Additionally, the multiplet intensity profiles may be influenced by the $^{63/65}\text{Cu}$ nuclear electric quadrupolar interactions as well as by the Euler angles, which relate the various interaction tensors to each other; however, the latter effects were neglected in the spin system simulations. The most striking feature of the present NMR results is the large chemical shift difference between P1 and P2 in **4** and **5**, but not in **6**. At first glance this result seems very surprising as the bonding connectivities of both sites are identical in all three compounds. This apparent discrepancy is most

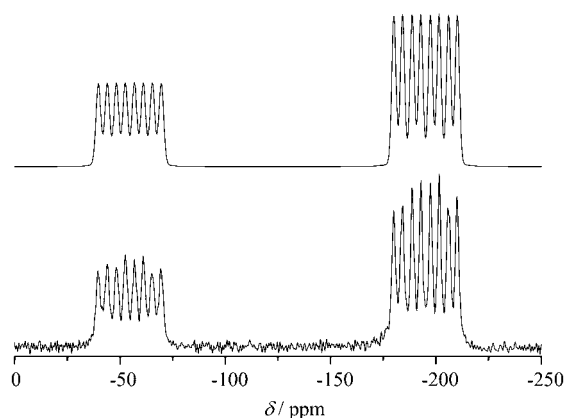


Figure 5. Experimental (bottom) and fitted (top) ^{31}P MAS-NMR (121.49 MHz, spinning speed 30 kHz) spectra of **4** (P1 –53.0 ppm; 1J (P,P) = 517 Hz, 1J (P,Cu) = 1040(1108) Hz, P2 –193.6 ppm; 1J (P,P) = 504 Hz, 1J (P,Cu) = 1042(1109) Hz; values for the ^{65}Cu isotope given in parentheses). Based on these results 1J (P,P) = 510 ± 7 Hz.

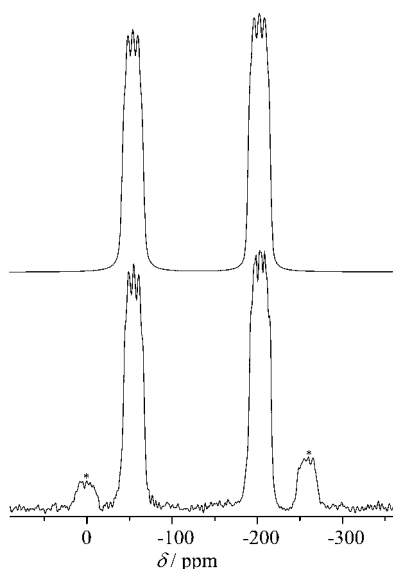


Figure 6. Experimental (bottom) and fitted (top) ^{31}P MAS-NMR (162.01 MHz; spinning speed 33 kHz) spectra of **5** (P1 -55.0 ppm; $^1J(\text{P,Cu})=968$ Hz, $^1J(\text{P,P})=605$ Hz, 47%, P2 -203.4 ppm; $^1J(\text{P,Cu})=1032$ Hz, $^1J(\text{P,P})=592$ Hz, 53%). Based on these results $^1J(\text{P,P})=598 \pm 7$ Hz.

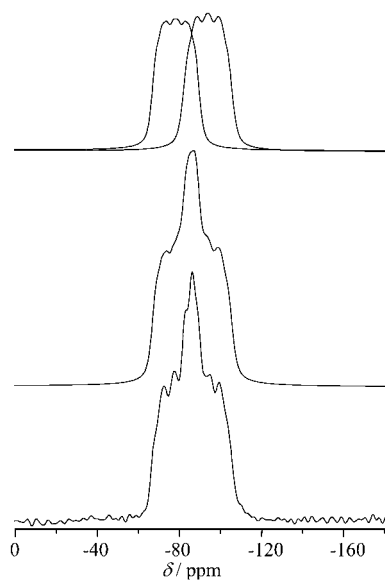


Figure 7. Experimental (bottom) and fitted (middle and top) ^{31}P MAS-NMR (162.01 MHz; spinning speed 33 kHz) spectra of **6** (P1 -78.2 ppm; $^1J(\text{P,Cu})=897$ Hz, $^1J(\text{P,P})=485$ Hz, 49%, P2 -93.8 ppm; $^1J(\text{P,Cu})=911$ Hz, $^1J(\text{P,P})=542$ Hz, 51%). Based on these results $^1J(\text{P,P})=514 \pm 30$ Hz.

likely a result of subtle differences in the arrangement of the Cp group and especially the CO ligands in each polymer and can be best interpreted when viewing the structures of the respective Cu_2P_4 rings as illustrated in Figure 8 in detail. In both the structures of **4** and **5** the downfield-shifted atom P1 is coordinated *trans* with respect to the Cp ligand of the Mo2 atom in **4** and the Mo1 atom in **5**, while the other Cp

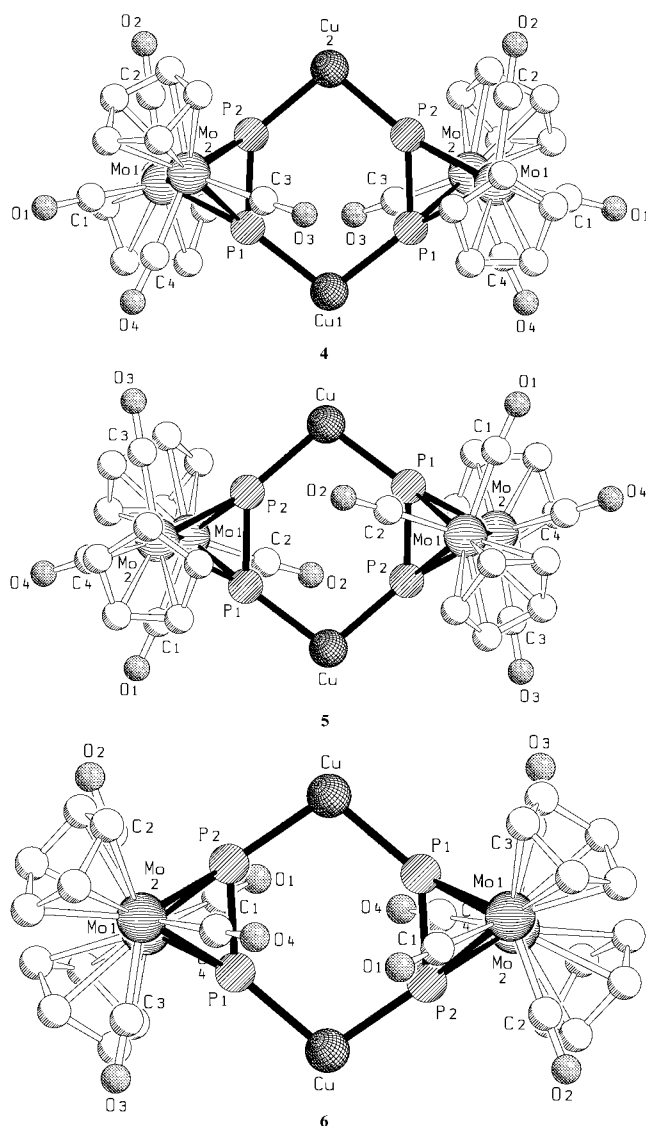


Figure 8. View of Cu_2P_4 rings of the polymers **4** (top, perpendicular to Cu1-P1-P1 plane), **5** and **6** (middle and bottom, respectively, both perpendicular to the P1-P2-P1-P2 plane). (Hydrogen and halogen atoms are omitted for clarity.)

ligand is *cis* oriented to it. In contrast the high-field shifted P2 atom has only *cis* oriented Cp ligands in both compounds. The situation is different in complex **6** in which the Cp ligands at the Mo atoms are *trans* oriented to both P1 and P2.

However, in compounds **4** and **5** the large chemical shift difference between the atoms P1 and P2 originates from the different orientations of these P atoms with respect to the CO ligands, whose large magnetic anisotropy results in a tremendous difference in shielding. This magnetic inequivalence is also evident from the $\text{C}_{\text{CO}}\cdots\text{P}$ interatomic distances listed in Table 3, which shows more carbonyl ligands in close proximity to P1 atoms than to P2, thus resulting in a downfield shift of the P1 atom. In contrast, the P1 and P2 atoms in **6** are flanked by the carbonyl ligands in almost the same relative orientation and show chemical shifts closer to those

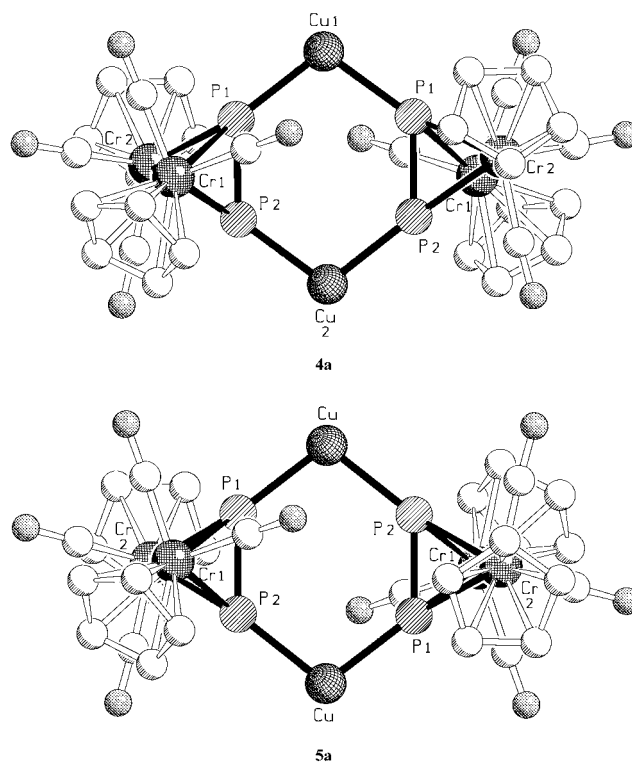
Table 3. $C_{Co}\cdots P$ interatomic distances of the compounds **4**, **5** and **6** [Å].

	4	5	6
C1...P1	3.561(2)	2.893(2)	3.169(4)
C2...P1	3.857(1)	2.776(3)	3.918(5)
C3...P1	2.811(3)	3.861(1)	2.741(2)
C4...P1	2.902(4)	3.512(2)	2.956(6)
C1...P2	3.832(3)	4.019(2)	2.889(6)
C2...P2	2.650(1)	3.131(3)	2.830(2)
C3...P2	3.203(2)	2.666(1)	3.889(5)
C4...P2	4.012(3)	3.805(2)	3.110(4)

of the P1 atoms in **4** and **5**. Furthermore, a closer look at the local symmetry of a repeat unit of **6** reveals an approximate C_{2h} symmetry. Accordingly, the ^{31}P chemical shifts observed in its NMR spectrum are nearly identical in this compound. To support the assignments proposed above, density functional theory (DFT) calculations were carried out by using model systems for **4** and **5** in which the Mo atoms were replaced by the lighter homologue Cr. This was done because for Mo and I, good quality all-electron basis and auxiliary basis sets are not available and calculations require use of the effective core potentials (ECP), which renders the calculation of ^{31}P NMR shielding constants for the original systems **4–6** not feasible.^[10] As the original systems are infinite polymer chains, molecular fragments containing three $[(\text{CuX})_2\{\text{Cp}_2\text{Cr}_2(\text{CO})_4(\mu,\eta^2-\eta^1-\text{P}_2)_2\}]$ ($X = \text{Cl}$ (**4a**), Br (**5a**)) units terminated with single X atoms were calculated. The symmetry point groups were found to be C_2 and C_i for **4a** and **5a**, respectively, and to reduce the influence of the terminal units in the following discussion only the central unit is considered (Figure 9). Table 4 presents the most important bond lengths of the calculated model compounds, which are independent of the metal atom, as well as the relevant experimental data. The structural parameters of the central $\text{Cu}_2\text{P}_4\text{X}_4$ unit are well reproduced, although most of the calculated bond lengths are slightly overestimated. As expected, the calculated P–Cr and Cr–Cr bond lengths are up to 0.09 Å shorter than the observed P–Mo and Mo–Mo distances.

For both **4a** and **5a**, the rings contain two pairs of symmetry-distinct P atoms. In **4a** the calculated ^{31}P isotropic shielding constants are 136 and 361 ppm for the P1 and P2 ligands, respectively, corresponding to chemical shifts of 78 and –147 ppm, while in **5a** the shielding constants are 141 ppm for P1 and 374 ppm for P2, corresponding to ^{31}P chemical shifts of 73 and –160 ppm, respectively. The downfield-shifted ^{31}P NMR resonances of the calculated Cr complex relative to those of the measured Mo polymers are not unexpected in view of experimental data on the complexes $[(\text{CpM}(\text{CO})_2)_2(\mu,\eta^2-\text{P}_2)]$ with $\delta = 111$ ppm for $M = \text{Cr}^{[11]}$ and $\delta = -41$ ppm for $M = \text{Mo}$.^[4] The results of these calculations thus support the deductions inferred from the structural and NMR spectral data concerning the polymers **4** and **5**.

^{63}Cu and ^{13}C MAS-NMR spectra of the compounds have also been recorded. For **6**, the ^{63}Cu MAS-NMR spectrum presents a sharp line centred near 399 ppm versus crystalline CuI; for **5** the MAS spectrum is strongly broadened by

Figure 9. View of the central rings of the model compounds **4a** and **5a** (hydrogen and halogen atoms are omitted for clarity).Table 4. Comparison of selected calculated and experimental bond lengths of the compounds **4**, **4a**, **5** and **5a** [Å].

	4	4a	5	5a
Cu–P	2.282, 2.304	2.305, 2.323	2.294, 2.300	2.314, 2.320
Cu–X	2.348, 2.360	2.384, 2.387	2.472, 2.481	2.488, 2.507
P–P	2.075	2.099	2.079	2.101

second-order quadrupolar perturbations. By using the DMFIT routine, the chemical shift and quadrupolar coupling constant can be estimated to be 560 ppm and 6.6 MHz respectively. No analysable ^{63}Cu MAS-NMR signal was obtained for **4**, presumably owing to extremely strong quadrupolar coupling. None of the compounds showed differentiable copper sites. Interestingly, two distinct Cp signals are observed in each of the ^{13}C CPMAS spectra of the polymers; $\delta = 91.1$ and 89.7 ppm for **4** and **5**, and $\delta = 88.9$ and 88.1 ppm for **6**. Fast ring rotation renders all of the C atoms of a given Cp ring magnetically equivalent.

Conclusion

It has been shown that the reaction of the P_2 ligand complex **1** with both Cu^{I} and Cu^{II} halides leads to the novel linear 1D polymeric compounds **4–6**, containing Cu^{I} complex centres. Evidently, the polymeric Cu^{I} complexes represent a

thermodynamic minimum in this system and the reduction of the Cu^{II} halides is forced.

Furthermore, the complex $[\{\text{CpMo}(\text{CO})_2\}_2(\mu, \eta^2\text{-P}_2)]$ has been demonstrated to be an effective linker unit for transition-metal centres. At first glance, the X-ray crystallographic studies show the same structural motifs for all these products: almost planar six-membered rings of P_4Cu_2 units that are linked by nearly orthogonally oriented planar Cu_2X_2 four-membered rings. However, a closer look at the structural details reveals that seemingly slight differences in the arrangement of both the Cp and especially the CO ligands in the solid-state structure influence the ³¹P NMR chemical shifts in their MAS-NMR spectra to a high degree. Thus, the influence of the cone of anisotropy of the CO ligands in **4** and **5** leads to a tremendous downfield shift of one of the P atoms, whereas in **6** both P atoms are influenced by the CO ligands in the same manner. These results are strongly supported by DFT calculations on the model compounds **4a** and **5a** in which Mo is substituted by its lighter homologue Cr. Thus, MAS-NMR spectroscopy is demonstrated to be a powerful tool providing invaluable information concerning the structural details of extended solid-state aggregates and networks.

Experimental Section

All manipulations were performed under an atmosphere of dry nitrogen using standard glove-box and Schlenk techniques. All solvents were freshly distilled from appropriate drying agents immediately prior to use. IR spectra were obtained on a BRUKER IFS280 spectrometer. ³¹P MAS-NMR spectra for **4** were recorded at 121.49 MHz using a spinning rate of 30 kHz and for **5** and **6** at 162.01 MHz using spinning rates of 33 kHz, on a Bruker DSX400 solid-state NMR spectrometer in a 2.5 mm probe. Typically, spectra were recorded by a rotor synchronised Hahn spin-echo sequence, generated with 90° pulse lengths of about 4 μs and relaxation delays of 3 minutes (280 scans). Chemical shifts were reported relative to 85% H₃PO₄. The spectral multiplets were simulated by using the Spinworks software package, taking both homo- and heteronuclear *J* coupling into account. For compound **4** the small difference between the magnetic moments of ⁶³Cu and the ⁶⁵Cu isotopes was explicitly taken into account, for **5** and **6** this effect was neglected, because of the overall low resolution observed. Since the ¹*J*(P,P) values were obtained by fitting the observed multiplets for each P site separately, the number to be quoted is represented by the average of both values. ⁶³Cu NMR spectra were recorded at 106.01 MHz by using single-pulse acquisition with short pulses of 1 μs length at spinning rates of 30–33 kHz. ¹³C NMR spectra were obtained by cross-polarisation applying standard conditions (1 ms contact time, 10 kHz MAS). Chemical shifts are reported relative to TMS.

All theoretical calculations were performed by using the TURBOMOLE program package.^[12,13] The functional theory (DFT) method along with the BP86 exchange-correlation functional was employed.^[14] To speed up calculations the Coulomb part was evaluated by using the MARI-J method.^[15,16] It is well-known that X-ray determined structures are usually not precise enough for calculations of chemical shifts, especially when light atoms such as H or C, or fast rotating ligands such as Cp, are present.^[17] Therefore, full structure optimisation within a given symmetry was performed for all systems using TZVP basis and auxiliary basis sets on all atoms.^[15,18] In the calculation of ³¹P chemical shifts within the GIAO approach,^[19] a more extended TZP basis set on P was used to increase the wave function flexibility in the core region. The TZP basis set or a basis set of similar quality is known to yield reasonably accurate NMR chemical shielding constants.^[18b,19,20] The ³¹P NMR chemical shifts relative

to 85% H₃PO₄ were calculated from absolute shielding constants σ by using P(OCH₃)₃ as an internal secondary standard ($\sigma = 74.3$) with an experimental ³¹P chemical shift of 140 ppm relative to 85% H₃PO₄.^[21]

Reagents: Unless otherwise stated, commercial grade chemicals were used. The complexes CuX were purified to remove traces of the Cu^{II} halides. $[\{\text{CpMo}(\text{CO})_2\}_2(\mu, \eta^2\text{-P}_2)]$ was synthesised according to the literature procedure.^[4]

Synthesis of 4: A solution of CuCl (40 mg, 0.4 mmol) in CH₃CN (10 mL) was added to a solution of **1** (100 mg, 0.2 mmol) in CH₃CN (10 mL) at room temperature and a red precipitate was formed immediately. The reaction mixture was stirred for another hour and the precipitate was isolated by filtration, washed with CH₃CN (3 × 25 mL) and dried under vacuum. Yield: 99 mg (83%). M.p.: 235–240 °C (decomp); IR (KBr): $\tilde{\nu} = 2006$ (vs), 1926 cm⁻¹ (vs; CO); elemental analysis calcd (%) for C₁₄H₁₀ClCuMo₂O₄P₂ (594.8): C 28.23, H 1.68; found: C 28.66, H 1.41.

Synthesis of 6-(CH₃CN)₂: A solution of CuI (72 mg, 0.4 mmol) in CH₃CN (10 mL) was added to a solution of **1** (100 mg, 0.2 mmol) in CH₃CN (10 mL) at room temperature and a red precipitate was formed immediately. The reaction mixture was stirred for another hour and the precipitate was isolated by filtration, washed with CH₃CN (3 × 25 mL) and dried under vacuum. Yield: 129 mg (90%); m.p.: 200–205 °C (decomp); IR (KBr): $\tilde{\nu} = 2270$ (m; CN), 1993 (vs), 1925 cm⁻¹ (vs; CO); elemental analysis calcd (%) for C₁₆H₁₃CuIMo₂N₂O₄P₂ (727.4): C 26.39, H 1.79, N 1.92; found: C 26.46, H 2.26, N 1.91.

Crystal structure analysis: Data were collected for complexes **4** and **6** on a STOE IPDS area-detector diffractometer by using AgK α ($\lambda = 0.56087$ Å) radiation. Machine parameters, crystal data and data collection parameters are summarised in Table 1. The structures were solved by direct methods by using SHELXS-97,^[22] full-matrix-least-squares refinement on *F*² in SHELXL-97^[23] with anisotropic displacement for non-H atoms, hydrogen atoms placed in idealised positions and refined isotropically according to the riding model.

CCDC-253102 and CCDC-253103 (**4** and **6**) contain the supplementary crystallographic data for this paper. These data can be obtained free of charge from the Cambridge Crystallographic Data Centre via www.ccdc.cam.ac.uk/data_request/cif.

Acknowledgements

This work was comprehensively supported by the Deutsche Forschungsgemeinschaft and the Fonds der Chemischen Industrie.

- [1] Review articles: a) P. J. Stang, B. Olenyuk, *Acc. Chem. Res.* **1997**, *30*, 502–518; b) D. Braga, F. Grepioni, G. R. Desiraju, *Chem. Rev.* **1998**, *98*, 1375–1405; c) O. M. Yaghi, H. Li, C. Davis, D. Richardson, T. L. Groy, *Acc. Chem. Res.* **1998**, *31*, 474–484; d) P. F. H. Schwab, M. D. Levin, J. Michl, *Chem. Rev.* **1999**, *99*, 1863–1933; e) S. Leininger, B. Olenyuk, P. J. Stang, *Chem. Rev.* **2000**, *100*, 853–908; f) M. J. Zaworotko, *Chem. Commun.* **2001**, 1–9; g) I. Manners, *Angew. Chem.* **1996**, *108*, 1712–1731; *Angew. Chem. Int. Ed. Engl.* **1996**, *35*, 1602–1621; h) M. O’Keeffe, M. Eddaoudi, H. Li, T. Reineke, O. M. Yaghi, *J. Solid State Chem.* **2000**, *152*, 3–20.
- [2] J. Bai, E. Leiner, M. Scheer, *Angew. Chem.* **2002**, *114*, 820–823; *Angew. Chem. Int. Ed.* **2002**, *41*, 783–786.
- [3] Compounds **4** and **5** have also been crystallised by layering a solution of the appropriate Cu^I halide in CH₃CN over a solution of **1** in toluene in the space group *C2/m* in which the Cp and CO ligands are disordered and occupy two equivalent positions. Compounds **4** and **5** thus appear to be isostructural when crystallising in this space group.
- [4] O. J. Scherer, H. Sitzmann, G. Wolmershäuser, *J. Organomet. Chem.* **1984**, *268*, C9–C12.
- [5] O. J. Scherer, H. Sitzmann, G. Wolmershäuser, *Angew. Chem.* **1984**, *96*, 979–980; *Angew. Chem. Int. Ed. Engl.* **1984**, *23*, 968–969.

- [6] M. Di Vaira, M. P. Ehses, M. Peruzzini, P. Stoppioni, *Polyhedron* **1999**, *18*, 2331–2336.
- [7] V. G. Albano, P. L. Bellon, G. Ciani, M. Manassero, *J. Chem. Soc. Dalton Trans.* **1972**, *2*, 171–175.
- [8] H. Negita, M. Hiura, Y. Kushi, M. Kuramoto, T. Okuda, *Bull. Chem. Soc. Jpn.* **1981**, *54*, 1247.
- [9] P. G. Eller, G. J. Kubas, R. R. Ryan, *Inorg. Chem.* **1977**, *16*, 2454–2462.
- [10] Calculations of NMR shielding constants in combination with ECPs are not implemented in the TURBOMOLE program package.
- [11] L. Y. Goh, C. K. Chu, R. C. S. Wong, *J. Chem. Soc. Dalton Trans.* **1989**, 1951–1956.
- [12] R. Ahlrichs, M. Bär, M. Häser, H. Horn, C. Kölmel, *Chem. Phys. Lett.* **1989**, *162*, 165–169.
- [13] O. Treutler, R. Ahlrichs, *J. Chem. Phys.* **1995**, *102*, 346–354.
- [14] a) A. D. Becke, *Phys. Rev. A* **1988**, *38*, 3098–3100; b) S. H. Vosko, L. Wilk, M. Nusair, *Can. J. Phys.* **1980**, *58*, 1200–1211; c) J. P. Perdew, *Phys. Rev. B* **1986**, *33*, 8822–8824; erratum: J. P. Perdew, *Phys. Rev. B* **1986**, *34*, 7406.
- [15] K. Eichkorn, O. Treutler, H. Öhm, M. Häser, R. Ahlrichs, *Chem. Phys. Lett.* **1995**, *242*, 652.
- [16] M. Sierka, A. Hogekamp, R. Ahlrichs, *J. Chem. Phys.* **2003**, *118*, 9136–9148.
- [17] M. Bühl, in *Encyclopedia of Computational Chemistry* (Eds.: P. von R. Schleyer, N. L. Allinger, T. Clark, J. Gasteiger, P. Kollman, H. F. Schaefer, P. R. Schreiner), Wiley, Chichester, **1998**, pp. 1835–1845.
- [18] a) A. Schäfer, H. Horn, R. Ahlrichs, *J. Chem. Phys.* **1992**, *97*, 2571–2577; b) A. Schäfer, C. Huber, R. Ahlrichs, *J. Chem. Phys.* **1994**, *100*, 5829–5835; c) K. Eichkorn, F. Weigend, O. Treutler, R. Ahlrichs, *Theor. Chem. Acc.* **1997**, *97*, 119–124.
- [19] G. Schreckenbach, T. Ziegler, *J. Phys. Chem.* **1995**, *99*, 606–611.
- [20] T. Helgaker, P. J. Wilson, R. D. Amos, N. C. Handy, *J. Chem. Phys.* **2000**, *113*, 2983–2989.
- [21] D. G. Gorenski, *Phosphorus ³¹NMR, Principles and Applications*, Academic Press, New York, **1984**.
- [22] G. M. Sheldrick, SHELXS-97, University of Göttingen, **1997**.
- [23] G. M. Sheldrick, SHELXL-97, University of Göttingen, **1997**.

Received: November 5, 2004
Published online: February 15, 2005